CMS Physics Analysis Summary

Contact: cms-pag-conveners-susy@cern.ch 2014/02/26

Search for top-squark pair production with Higgs and Z bosons in the final state in pp collisions at $\sqrt{s} = 8$ TeV

The CMS Collaboration

Abstract

A search for direct top-squark pair production with Higgs or Z bosons in the decay final state is performed using a data sample of proton-proton collisions at $\sqrt{s} = 8$ TeV, collected by the CMS detector at the LHC that corresponds to an integrated luminosity of 19.5 fb^{-1}. The search is performed in a sample of events containing leptons and b jets. No evidence for a significant excess of events over the standard model background prediction is observed. The results are interpreted in the context of simplified models with pair production of a heavier top-squark mass eigenstate $\tilde{t}_2$ decaying to a lighter top-squark mass eigenstate $\tilde{t}_1$ via either $\tilde{t}_2 \to H\tilde{t}_1$ or $\tilde{t}_2 \to Z\tilde{t}_1$, followed in both cases by $\tilde{t}_1 \to t\tilde{\chi}^0_1$. The interpretation is performed in the region of signal mass parameter space $m_{\tilde{t}_1} - m_{\tilde{\chi}^0_1} \sim m_t$, which so far is not probed by existing searches for direct top-squark pair production. The analysis excludes top squarks with masses $m_{\tilde{t}_2} < 575$ GeV and $m_{\tilde{t}_1} < 400$ GeV at the 95% confidence level.

1 Introduction

Supersymmetry (SUSY) with R-parity conservation is an extension to the standard model (SM) that provides a candidate particle for dark matter and addresses the gauge hierarchy problem [1–6]. This problem originates in the spin 0 nature of the Higgs (H) boson, whose mass squared is subject to quadratic divergences from higher order corrections. The leading divergent contribution from SM particles arises from the H boson coupling to the top quark. A possible mechanism to stabilize the H boson mass is the existence of a scalar top quark with a mass not too different from that of the top quark [7–11]. Searches for direct top-squark production from the ATLAS [12–15] and CMS [16] collaborations have focused mainly on the simplest scenario, in which only the lightest top-squark mass eigenstate, $\widetilde{\mathrm{t}}_1$, is accessible. In these searches, the top-squark decay modes considered are top plus neutralino, $\widetilde{\mathrm{t}}_1 \to \mathrm{t}\widetilde{\chi}_1^0 \to \mathrm{bW}\widetilde{\chi}_1^0$, or bottom plus chargino, $\widetilde{\mathrm{t}}_1 \to \mathrm{b}\widetilde{\chi}_1^+ \to \mathrm{bW}\widetilde{\chi}_1^0$. These two decay modes are expected to have large branching fractions if kinematically allowed. The lightest neutralino, $\widetilde{\chi}_1^0$, is the lightest supersymmetric particle in the (R-parity conserving) models considered; the experimental signature of such a particle is missing transverse energy ($E_{\mathrm{T}}^{\mathrm{miss}}$) in the detector.

Searches for top-squark pair production are challenging because the cross section is approximately six times smaller than that for $\mathrm{t\bar{t}}$ production if $m_{\widetilde{\mathrm{t}}_1} \sim m_{\mathrm{t}}$ and decreases rapidly with increasing top-squark mass. When the mass difference between the top squark and the $\widetilde{\chi}_1^0$ is large, top-squark production can be distinguished from $\mathrm{t\bar{t}}$ production by using events with extreme kinematic features, especially large $E_{\mathrm{T}}^{\mathrm{miss}}$. This strategy is being pursued in existing searches and has sensitivity to top-squark masses up to about 650 GeV for low $\widetilde{\chi}_1^0$ masses. There are, however, regions of parameter space in which existing searches have limited sensitivity. In the regions where the mass difference is roughly equal to the top quark mass, $m_{\widetilde{\mathrm{t}}_1} - m_{\widetilde{\chi}_1^0} \sim m_{\mathrm{t}}$, the kinematic distributions of the signal processes are similar to those for SM top-quark pair production [17]. This region of phase space can be targeted using events with topologies where top-squark events can be distinguished from the $\mathrm{t\bar{t}}$ background. An example is gluino pair production where the gluino decays to top squarks, giving rise to a signature with four top quarks in the final state [18, 19].

This analysis also targets the region of phase space where $m_{\widetilde{\mathrm{t}}_1} - m_{\widetilde{\chi}_1^0} \sim m_{\mathrm{t}}$ by focusing on signatures of $\mathrm{t\bar{t}HH}$, $\mathrm{t\bar{t}HZ}$, and $\mathrm{t\bar{t}ZZ}$, using a sample of events with a modest requirement on $E_{\mathrm{T}}^{\mathrm{miss}}$. These final states can arise from the pair production of the heavier top-squark mass eigenstate $\widetilde{\mathrm{t}}_2$, which decays to $\widetilde{\mathrm{t}}_1$ and a H or Z boson. The $\widetilde{\mathrm{t}}_1$ is subsequently assumed to decay to $\mathrm{t}\widetilde{\chi}_1^0$. These processes are shown in Fig. 1. These final states can arise in other scenarios, such as $\widetilde{\mathrm{t}}_1 \to \mathrm{t}\widetilde{\chi}_2^0$ with $\widetilde{\chi}_2^0 \to \mathrm{H}\widetilde{\chi}_1^0$ or $\widetilde{\chi}_2^0 \to \mathrm{Z}\widetilde{\chi}_1^0$. The analysis is also sensitive to a range of models in which the lightest supersymmetric particle is a gravitino [20]. The relative branching fractions for modes with H and Z are model-dependent, so it is useful to search for both decay modes.

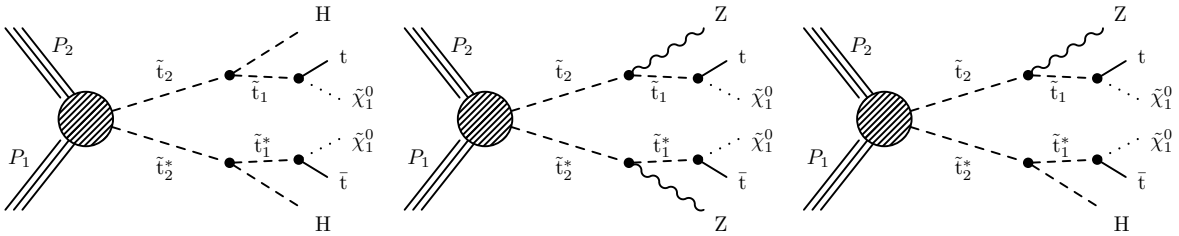

Figure 1: Diagram for the heavier top squark $\widetilde{\mathrm{t}}_2$ pair production, where $\widetilde{\mathrm{t}}_2 \to \mathrm{H}\widetilde{\mathrm{t}}_1$ or $\widetilde{\mathrm{t}}_2 \to \mathrm{Z}\widetilde{\mathrm{t}}_1$ and the lightest top squark subsequently decays $\widetilde{\mathrm{t}}_1 \to \mathrm{t}\widetilde{\chi}_1^0$. The symbol * denotes charge conjugation.

In the signal model considered, $\widetilde{t}_2$ is assumed always to decay to $\widetilde{t}_1$ in association with a H or a Z boson, such that $\mathcal{B}(\widetilde{t}_2 \to H\widetilde{t}_1) + \mathcal{B}(\widetilde{t}_2 \to Z\widetilde{t}_1) = 100\%$. Other possible decay modes are $\widetilde{t}_2 \to t\widetilde{\chi}_1^0$ and $\widetilde{t}_2 \to b\widetilde{\chi}_1^+$. These alternative decay modes are not considered here, since they give rise to final states that are covered by existing searches for direct top-squark pair production [12–16].

The current search for $\widetilde{t}_2$ production is performed using a sample of events with leptons (electrons or muons) and jets identified as originating from b quarks (b jets). Three main search channels are used: (i) either one lepton or two leptons with opposite-sign charge (OS), together with at least three b jets, (ii) two leptons of the same-sign charge (SS) and (iii) at least three leptons, where the SS and three lepton selections are accompanied by at least one b jet. These requirements suppress background contributions from top quark pair production, which has two b quarks and either one or two OS leptons from the $t\bar{t} \to \ell\nu jjb\bar{b}$ or $t\bar{t} \to \ell\nu\ell\nu b\bar{b}$ decay modes. Here ℓ corresponds to an electron (e) or muon (μ) and j to a quark. The sensitivity to the signal arises both from events with additional b quarks in the final state (mainly from $H \to b\bar{b}$), and from events with additional leptons, such as leptonically decaying Z bosons or W bosons from the $\widetilde{t}_2$ decay, or from $H \to W^+W^-$ and $H \to ZZ$ events. The results are based on data collected at $\sqrt{s} = 8$ TeV by the CMS experiment at the LHC during 2012, corresponding to an integrated luminosity of $19.5\,\text{fb}^{-1}$.

The paper is organized as follows: Section 2 presents the event samples and the object selections used. Section 3 describes the search regions and Section 4 details the background estimation methods. The experimental results are presented in Section 5, and in Section 6 we discuss the interpretation of the results in the context of the signal model of the pair production of a heavier top-squark mass eigenstate $\widetilde{t}_2$ decaying to a lighter top-squark mass eigenstate $\widetilde{t}_1$.

2 Event samples and object selection

The data used for this search were collected with the high p_T electron (e) or muon (μ) single-lepton trigger, which requires at least one e with transverse momentum $p_T > 27$ GeV or μ with $p_T > 24$ GeV, or with the ee, eμ, or $\mu\mu$ double-lepton triggers, which require at least one e or one μ with $p_T > 17$ GeV and another with $p_T > 8$ GeV. Events are also acquired with a double-lepton trigger targeting lower p_T leptons, requiring $p_T > 8$ GeV, but with an additional online selection of $H_T \equiv \Sigma_{jet}|p_T^{jet}| > 175$ GeV, considering only jets with $p_T > 40$ GeV in the sum.

Events are reconstructed offline using the particle-flow (PF) technique [21, 22]. Electron candidates are reconstructed by associating tracks with energy clusters in the electromagnetic calorimeter [23]. Muon candidates are reconstructed by combining information from the tracker and the muon detectors [24]. Signal leptons are produced in the decays of W and Z bosons. In order to distinguish these leptons from those produced in the decays of heavy-flavor hadrons, all lepton candidates are required to be compatible with originating from the primary interaction vertex and to have small transverse impact parameter with respect to this vertex. Furthermore, since misidentified lepton candidates arising from background sources such as the decays of hadrons are typically embedded in jets, all lepton candidates are required to be isolated from hadronic activity in the event. This is achieved by imposing a maximum allowed value on the scalar sum of the p_T of charged and neutral hadrons and photons within a cone of $\Delta R \equiv \sqrt{\Delta\eta^2 + \Delta\phi^2} < 0.3$ around the lepton candidate momentum direction at the origin. The surrounding hadronic activity is corrected for the energy contribution from additional proton-proton interactions in the event (pileup), as described in Ref. [25].

Jets are constructed using the anti-k_T clustering algorithm [26] with a distance parameter of 0.5.

The energies of reconstructed jets are corrected for residual non-uniformity and nonlinearity of the detector response using corrections based on exclusive dijet and γ/Z+jet data [27]. The energy contribution from pileup is estimated using the jet area method [28] for each event and is subtracted from the jet p_T. Only high p_T jets in the central calorimeter $|\eta| < 2.4$ are considered. Jets consistent with the decay of heavy-flavor hadrons are identified by the combined secondary vertex b-tagging algorithm using the medium and loose working points, which have tagging efficiencies of 70% and 80–85%, and misidentification rates for light flavor jets less than 2% and 10%, respectively [29]. The E_T^{miss} is calculated as the magnitude of the vector sum of the transverse momenta of all PF particles, incorporating jet energy corrections. Quality requirements are applied to remove a small fraction of events in which detector effects such as electronic noise can affect the E_T^{miss} reconstruction. Events are required to have $E_T^{miss} > 50$ GeV to reduce background contributions from sources with a single W boson and from jet production via QCD processes.

Simulated event samples are used to study the characteristics of the signal and to calculate its acceptance, as well as for part of the SM background estimation. Pair production of $\widetilde{t}_2$ is generated with MADGRAPH 5 [30], including up to two additional partons at the matrix element level, which are matched to the parton showering from PYTHIA [31]. The SUSY particle decays are simulated with PYTHIA 6.424 with a uniform amplitude over phase space [32]. The decay modes considered (see Fig. 1) are assumed to have a branching fraction of unity when limits are set on masses. The H boson mass is set to 125 GeV [33] and branching fractions are set according to the corresponding expectations from the SM [34]. For each decay mode, a grid of signal events is generated as a function of the two top-squark masses $m_{\widetilde{t}_2}$ and $m_{\widetilde{t}_1}$. The $\widetilde{t}_1$ is forced to decay to top plus neutralino assuming $m_{\widetilde{t}_1} - m_{\widetilde{\chi}_1^0} = 175$ GeV. The signal event rates are normalized to cross sections calculated at next-to-leading order (NLO) in the strong coupling constant, including the resummation of soft gluon emission at next-to-leading-logarithmic accuracy (NLO+NLL) [35–40].

The SM background processes considered are the production of $t\bar{t}$; $t\bar{t}$ in association with a boson (H, W, Z, γ^*); W, Z, and γ^* + jets; triboson; diboson; single top quark in the s, t, and tW channels; and single top quark in association with an additional quark and a Z boson. These processes are generated with MADGRAPH, POWHEG [41] or MC@NLO [42, 43], using the CT10 [44] (POWHEG), CTEQ6M [45] (MC@NLO), and CTEQ6L1 [45] (MADGRAPH) parton distribution functions. SM background event rates are normalized to cross sections [42, 43, 46–51] calculated at next-to-next-to-leading order (NNLO) when available, otherwise at NLO. The generated signal samples are processed with the parametric simulation of the CMS detector [52], while all the background samples use the full simulation of the CMS detector based on GEANT4 [53].

3 Search regions

The search consists of a set of counting experiments in disjoint signal regions targeting the signatures shown in Fig. 1, while suppressing the contributions from SM backgrounds, predominantly $t\bar{t}$. Events are classified according to the lepton multiplicity and charge requirements on the leptons. Three main categories of events are considered.

The definitions of the search regions are given in summary form in Table 1, and detailed in the following subsections. The first includes events with one lepton or two OS leptons. Since these lepton signatures also arise in the decays of top quark pairs, requirements of at least three b jets are used to suppress this background. The other two categories are events with exactly two SS leptons, and events with three or more leptons, which do not typically arise in $t\bar{t}$ events.

A requirement of at least one b jet is applied, primarily to further suppress the contribution from backgrounds with W and Z bosons. Lepton vetos are used to ensure that the three main categories of events are non-overlapping.

3.1 Selection with a single lepton or two opposite-sign charge leptons

The signal categories with one lepton or two OS leptons, accompanied in either case by at least three b jets target signatures with H bosons, which have a large branching fraction for $H \to b\bar{b}$. In the single lepton channel, events are required to have exactly one e with $p_T > 30$ GeV and $|\eta| < 1.4442$ or exactly one μ with $p_T > 25$ GeV and $|\eta| < 2.1$. Events with an indication of an additional lepton, either an isolated track or a hadronic τ lepton candidate [54], are rejected in order to reduce the background from $t\bar{t}$ events in which both W bosons decay leptonically ($t\bar{t} \to \ell\ell + \text{jets}$). In the double lepton channel, events are required to have exactly two e or μ (ee, eμ, or $\mu\mu$) with $p_T > 20$ GeV and $|\eta| < 2.4$. In this case, events with an additional e or μ with $p_T > 10$ GeV are rejected. Any electron candidate in the region $1.442 < |\eta| < 1.566$, a less well instrumented transition region between the barrel and endcap calorimeter, is excluded in the event selection. Jets must be separated in space from the candidate leptons by $\Delta R > 0.4$.

In these search categories, a typical $t\bar{t}$ background event has two b jets in the final state, while signal events could have up to four additional b jets, two from each H decay. The requirement of more than two b jets greatly suppresses the $t\bar{t}$ background contribution. For events with three b jets, the p_T threshold applied is 40 GeV; for events with at least four b jets, the threshold is lowered to 30 GeV. In both cases, the medium working point of the b jet-tagger is used (see Section 2). To further reduce the $t\bar{t}$ background contribution in the sample with exactly three b jets, events are required to have at least five jets and a fourth b jet satisfying the loose but not the medium working point of the tagger. Signal events can have large jet multiplicities, while in the case of the $t\bar{t}$ background, additional jets are needed to satisfy this selection criterion. To reduce the contribution of jets from pileup in the event, a requirement is applied on a multivariate discriminant incorporating the multiplicity of objects clustered in the jet, the jet shape, and the compatibility of the charged constituent of the jet with the primary interaction vertex.

Besides the requirements listed above, the analysis in the single lepton channel further selects events with large transverse mass of the nominal (ℓ, ν) system, defined as
$m_T \equiv \sqrt{2p_T^\ell p_T^\nu (1 - \cos(\phi^\ell - \phi^\nu))}$, where the p_T of the selected lepton is used and the (x, y)

Table 1: Summary of the signal region definitions for the different selections, specified by rows in the table. The signal regions correspond to all possible combinations of requirements in each row, where different regions for the kinematic variables are separated by commas.

N_ℓ	Veto	$N_{\text{b jets}}$	N_{jets}	E_T^{miss} [GeV]	Additional requirements [GeV]
1	track or τ_h	$= 3$ ≥ 4	≥ 5 ≥ 4	≥ 50	$m_T > 150$ $m_T > 120$
2 OS	extra e/μ	$= 3$ ≥ 4	≥ 5 ≥ 4	≥ 50	($N_{bb} = 1$ with $100 \leq m_{bb} \leq 150$), $N_{bb} \geq 2$
2 SS	extra e/μ	$= 1$ ≥ 2	$[2, 3]$, ≥ 4	$[50, 120]$, ≥ 120	for low/high-p_T: $H_T \in [200, 400]$, ≥ 400
≥ 3	—	$= 1$ $= 2$ ≥ 3	$[2, 3]$, ≥ 4 ≥ 3	$[50, 100]$, $[100, 200]$, ≥ 200	for on/off-Z: $H_T \in [60, 200]$, ≥ 200

components of the neutrino momentum are equated to the corresponding $E_{\mathrm{T}}^{\mathrm{miss}}$ components. For events in which the $E_{\mathrm{T}}^{\mathrm{miss}}$ arises from a single neutrino from a W boson decay, this variable has a kinematic endpoint $m_{\mathrm{T}} < m_{\mathrm{W}}$, where m_{W} is the W mass. The requirement of large m_{T} ($m_{\mathrm{T}} > 150$ GeV for events with three b jets or $m_{\mathrm{T}} > 120$ GeV for events with at least four b jets) provides strong suppression of the semileptonic $\mathrm{t\bar{t}}$ background ($\mathrm{t\bar{t}} \to \ell + \text{jets}$).

The study of the OS dilepton channel uses the information from pairs of b jets that satisfy kinematic requirements intended to identify pairs consistent with a $\mathrm{H} \to \mathrm{b\bar{b}}$ decay: $\Delta R_{\mathrm{bb}} \leq 2\pi/3$, $m_{\mathrm{bb}}/[p_{\mathrm{T}}^{\mathrm{bb}} \cdot \Delta R_{\mathrm{bb}}] \leq 0.65$, and $|\Delta y_{\mathrm{bb}}| \leq 1.2$, where y is the rapidity. Only b jets satisfying the medium working point of the tagger are used to select bb combinations. The signal sample is then selected by applying a requirement on either the number of selected bb pairs (N_{bb}) or on the invariant mass of the bb system (m_{bb}). Events are required to have one selected b jet pair with $100 \leq m_{\mathrm{bb}} \leq 150$ GeV or at least two selected b jet pairs. For the signal models of interest, particularly the $\tilde{\mathrm{t}}_2 \to \mathrm{H}\tilde{\mathrm{t}}_1$ decay mode, the signal regions with largest b jet multiplicity (≥ 4 b jets) have the best sensitivity.

3.2 Selection with two same-sign charge leptons

The signal regions with two SS leptons also target signatures with multiple sources of leptons. Events from SM processes with two SS leptons are extremely rare. The analysis for this event category follows closely that described in Ref. [55]. The only difference is the addition of a veto on events containing a third lepton, to remove the overlap with the three lepton event category. These signal regions recover events in which one of the three leptons falls outside the detector acceptance and selection criteria. Multiple signal regions are also defined for the sample of two SS leptons, based on jet and b jet multiplicities, $E_{\mathrm{T}}^{\mathrm{miss}}$, and H_{T}, and on whether the leptons with $|\eta| < 2.4$ satisfy $p_{\mathrm{T}} > 10$ GeV (low–p_{T} analysis) or $p_{\mathrm{T}} > 20$ GeV (high–p_{T} analysis). Also, a baseline selection is introduced, which requires at least two jets, moderate H_{T} (> 250 GeV in the low–p_{T} analysis and > 80 GeV in the high–p_{T} analysis), and moderate $E_{\mathrm{T}}^{\mathrm{miss}}$ (> 30 GeV for events with $H_{\mathrm{T}} < 500$ GeV; otherwise, there is no $E_{\mathrm{T}}^{\mathrm{miss}}$ requirement).

3.3 Selection with three leptons

The signal regions with at least three leptons and at least one b jet are sensitive to all of the processes shown in Fig. 1. These processes have many sources of leptons, such as Z bosons from the top-squark decays, and W and Z bosons from H boson decays. Even though signatures giving rise to three leptons correspond to processes with low branching fractions, this channel has good sensitivity because the backgrounds are strongly suppressed. The dataset is acquired using the double lepton triggers. Events are selected offline with at least three e or μ with $p_{\mathrm{T}} > 10$ GeV, including at least one with $p_{\mathrm{T}} > 20$ GeV, and $|\eta| < 2.4$. Events with two leptons of opposite-sign charge with an invariant mass below 12 GeV are removed from the sample to reduce the contribution of leptons originating from low-mass bound states.

The largest SM background with a trilepton signature is WZ+jets production, which is highly suppressed by the b jet requirement. Events are required to have at least two jets with $p_{\mathrm{T}} > 30$ GeV and at least one b jet satisfying the medium working point of the tagger. Leptons within $\Delta R < 0.4$ of a b jet are not considered isolated and are merged with the original b jet. This requirement imposes an additional isolation criterion for leptons and reduces the dominant background, $\mathrm{t\bar{t}}$ production, by 25–40% depending on the search region, compared to the case where such an object is reconstructed as a lepton rather than a b jet. The efficiency for signal leptons is reduced by 1%.

This three-lepton event sample is divided into several search regions by imposing requirements

on the jet and b jet multiplicity, $E_{\mathrm{T}}^{\mathrm{miss}}$, and the hadronic activity in the event, as given by the kinematic variable H_{T}. Finally, events are classified as either on-Z, if there is a pair of leptons of the same flavor and opposite-sign charge with an invariant mass within 15 GeV of the Z boson mass, or off-Z, if no such pair exists or if the invariant mass is outside this range.

The separation of events into these samples improves the sensitivity of the search. For the signal models of interest, the signal regions with large b jet multiplicity (those designated $\mathrm{N_{b\,jets}}$=2 and $\mathrm{N_{b\,jets}}\geq$3), as well as high $E_{\mathrm{T}}^{\mathrm{miss}}$ and high H_{T}, provide the best sensitivity. For the $\tilde{\mathrm{t}}_2 \to \mathrm{Z}\tilde{\mathrm{t}}_1$ decay mode, particularly where the Z bosons are kinematically allowed to be on shell, the on-Z regions are the most sensitive, while in the case of off-shell Z boson decays and for the $\tilde{\mathrm{t}}_2 \to \mathrm{H}\tilde{\mathrm{t}}_1$ decay mode, the off-Z regions have more sensitivity.

4 Background estimation

The main background in all search regions arises from SM $\mathrm{t\bar{t}}$ events, which usually have two b jets and at most two isolated leptons of opposite-sign charge from W boson decays. Thus, $\mathrm{t\bar{t}}$ events can only satisfy the selection criteria if accompanied by sources of additional b jets or leptons. Such backgrounds are estimated using control samples in data, as described below. This method greatly reduces the dependence of the background prediction on the accurate modeling in simulation, on the knowledge of the inclusive $\mathrm{t\bar{t}}$ production cross-section, on the integrated luminosity, and on the object selection efficiencies.

Additional backgrounds arise from processes involving one or more W and Z bosons, though these contributions are suppressed by b jet requirements. Finally, all event categories have backgrounds from rare SM processes, such as $\mathrm{t\bar{t}Z}$ and $\mathrm{t\bar{t}W}$, whose cross sections have not been precisely measured experimentally [56]. The prediction for these contributions is derived from simulation, and a systematic uncertainty of 50% is assigned to account for the uncertainty in the NLO calculations of their cross sections. The rest of this section describes the background predictions for each of the specific event categories.

4.1 Backgrounds in selections with a single lepton or two opposite-sign charge leptons

For the single lepton or two OS lepton signal regions, the dominant background is from $\mathrm{t\bar{t}}$ events (85–95% of the total). These events can have at least three b jets when $\mathrm{t\bar{t}}$ is produced with additional jets that may be mistagged in the case of light-parton jets or that may contain real b mesons from radiation that splits into $\mathrm{b\bar{b}}$ pairs. In the case of $\mathrm{t\bar{t}} \to \ell + \text{jets}$ events, there are small additional contributions from $\mathrm{W} \to \mathrm{c\bar{s}}$ decays, with a mistag, and from the rare $\mathrm{W} \to \mathrm{c\bar{b}}$ decay mode; in the case of $\mathrm{t\bar{t}} \to \ell\ell + \text{jets}$ events, τ leptons from the second W boson decay that are misidentified as b jets also contribute. In the modeling of these sources of additional b jets in $\mathrm{t\bar{t}}$ events there are imperfections. Scale factors are used to normalize the background prediction from simulation to the rates observed in data. For each signal region, the corresponding scale factor is derived in a control region enhanced in background $\mathrm{t\bar{t}}$ events. The control regions for the single lepton selections are defined by inverting the m_{T} requirement ($50 \leq m_{\mathrm{T}} \leq 100$ GeV), while in the OS dilepton case, the control sample is defined by inverting the m_{bb} and N_{bb} requirements ($N_{\mathrm{bb}} = 0$, or $N_{\mathrm{bb}} = 1$ with $m_{\mathrm{bb}} \leq 100\,\mathrm{GeV}$ or $m_{\mathrm{bb}} \geq 150\,\mathrm{GeV}$). The contribution from non-$\mathrm{t\bar{t}}$ events is estimated from simulation and subtracted from the data before deriving the normalization. To reduce the contribution from a possible signal in these control regions, the samples are restricted to events with low jet multiplicity: for the three b jet category, only events with exactly five jets are used, and for the category with at least four b jets, only events with exactly four jets are used. The dominant source of uncertainty for

the background prediction arises from the statistics of the control sample (15-35% on the total background). The $\mathrm{t\bar{t}}$ background prediction also depends on the ratio of events in the signal and control regions, which is evaluated in simulation. The modeling of the extrapolation in m_{T} for the one lepton case or m_{bb} and N_{bb} for the case of two OS leptons is validated in control samples obtained by selecting events with fewer than three b jets, which corresponds predominantly to $\mathrm{t\bar{t}}$ events.

In the single lepton channel, the modeling of the high m_{T} tail is critical for the background estimation. True semileptonic $\mathrm{t\bar{t}}$ events have an endpoint at $m_{\mathrm{T}} \approx m_{\mathrm{W}}$, with $E_{\mathrm{T}}^{\mathrm{miss}}$ resolution effects primarily responsible for populating the $m_{\mathrm{T}} > m_{\mathrm{W}}$ tail. The simulation of $E_{\mathrm{T}}^{\mathrm{miss}}$ resolution effects in the m_{T} tail is investigated by selecting events with one or two b jets and by varying the number of additional jets. The comparison of simulation to data is used to extract scale factors and uncertainties for the semileptonic $\mathrm{t\bar{t}}$ prediction. The scale factors are in the range 1.1–1.2, depending on the m_{T} requirement, with corresponding uncertainties of 5–10%. The semileptonic background contributes 50–60% of the total background in the single lepton signal regions. Events from $\mathrm{t\bar{t}} \to \ell\ell +$ jets can also satisfy the single lepton event selection if the second lepton is not identified or is not isolated and can give rise to large values of $E_{\mathrm{T}}^{\mathrm{miss}}$ and m_{T} due to the presence of two neutrinos. This $\mathrm{t\bar{t}} \to \ell\ell +$ jets contribution comprises $\sim$30–40% of the total background and is derived from simulation, with a scale factor and uncertainty determined from a comparison of data and simulation in the dilepton control region.

In the channels with two OS leptons, the most important issues in the background prediction are related to the construction of b jet pairs (see Section 3.1 for the full list of requirements). Physics modeling of both emission of extra radiation leading to jets and gluon splitting to $\mathrm{b\bar{b}}$, as well as algorithmic effects, such as τ or charm mistagging and the b jet identification efficiency, can affect the m_{bb} variable. The modeling of these effects is validated in the high-statistics single lepton m_{T} control sample, where the m_{bb} distributions in data and simulation are compared as a function of the b jet multiplicity. These studies are used to derive uncertainties for the extrapolation factors in the dilepton channel, corresponding to 20–30% of the total background.

4.2 Backgrounds in selections with two same-sign charge leptons

For the signal regions with two SS leptons, the background estimates and uncertainties are derived following the procedures described in Ref. [55]. There are three main categories of backgrounds. Non-prompt leptons are produced from heavy-flavor decays, misidentified hadrons, muons from decays in flight of light mesons, or electrons from unidentified photon conversions. Charge misidentification arises mainly from electrons that suffer severe bremsstrahlung in the tracker material and so that the charge is misreconstructed. Finally, rare SM processes yielding two genuine SS leptons can contribute significantly, especially in signal regions with tight requirements. Backgrounds from non-prompt leptons and rare SM processes dominate, each contributing 20–80% of the total, while charge misidentification contributes 1–5%.

The background from non-prompt leptons is evaluated with a sample in data where at least one lepton fails the full identification criteria but passes a combination of relaxed isolation and lepton-identification requirements. The number of events in this sample is scaled by the probability of a loosely identified lepton to pass the full set of selection requirements. The charge misidentification background is obtained from the opposite-sign ee or eμ events passing the full kinematic selection weighted by the p_{T}- and η-dependent probability of electron charge misassignment. The systematic uncertainty on the total background prediction is driven by the uncertainty on the contribution from rare SM processes and on the rate of events with a jet mis-identified as a prompt lepton (30–50% on the total background).

4.3 Backgrounds in selections with three leptons

For signal regions with at least three leptons, there are two main types of backgrounds. In signal regions without a Z candidate, the background with two prompt leptons and an additional object mis-identified as a prompt lepton dominates, comprising 50–90% of the total. In signal regions with a Z candidate, the dominant background is typically from SM processes with at least three genuine prompt leptons, corresponding to 60–100% of the total.

The background sources with two leptons from W or Z boson decays and a third object misidentified as a prompt lepton are predominantly from $\mathrm{t\bar{t}}$ production, though Z + jets and WW + jets also contribute. The procedure to estimate this background contribution follows closely that used for the analysis of events with two leptons of the same-sign charge [55]. The probability for a lepton from the decay of a b hadron to satisfy the analysis selection criteria is measured in a data sample enriched in QCD dijet events. This probability is applied to a sample of three-lepton events, in which the isolation requirement on one of the leptons is removed, providing an estimate of the background contribution from non-prompt leptons. A systematic uncertainty of 30% is derived for this background based on studies of the method in simulation. This uncertainty accounts for the difference in the p_{T} spectrum of b jets in the control sample, where the probability is measured, compared to the spectrum in the signal sample, where it is applied. This systematic uncertainty dominates the uncertainty on the background prediction in the signal regions with looser kinematic requirements. Signal regions with tight kinematic requirements also have a significant statistical uncertainty due to the size of the sample used to derive this background estimate. These are the dominant sources of uncertainty on the backgrounds in the off-Z signal regions (20–90% on the total background).

The background contribution from events with two vector bosons that produce three genuine prompt isolated leptons, mainly WZ + jets and ZZ + jets, is estimated from simulation and is validated by comparing data and simulation in a control sample in which the full selection is applied and the b jet requirement is inverted. A control sample enhanced in the WZ background is obtained by selecting events with three high-p_{T} leptons. One pair of leptons is required to form a $\mathrm{Z} \to \ell^+\ell^-$ candidate. The third lepton is combined with the $E_{\mathrm{T}}^{\mathrm{miss}}$ vector, and this system is required to form a W candidate ($50 < E_{\mathrm{T}}^{\mathrm{miss}} < 100$ GeV and $50 < m_{\mathrm{T}} < 120$ GeV). Another control sample, enhanced in the ZZ background, is obtained by selecting events with four leptons and $E_{\mathrm{T}}^{\mathrm{miss}} < 50$ GeV. Two leptons are required to form a Z candidate. A scale factor is derived for the ZZ background prediction based on the comparison of data and simulation in this sample. The systematic uncertainty on the diboson background is derived based on these comparisons, which are limited by the statistical precision of the control samples. A 50% uncertainty is assigned to account for possible mismodeling of additional partons required to satisfy the b jet requirement.

5 Results

The results of the search are shown in Tables 2, 3, and 4, and in Figs. 2, 3, and 4. For the event selections with one lepton, Fig. 2 (top) shows a comparison of the m_{T} distribution in data and simulation. The sample at low m_{T} is enhanced in semileptonic $\mathrm{t\bar{t}}$ events and is the control region used to derive the normalization for this background contribution. In this region, the simulation is used to model the m_{T} shape for the $\mathrm{t\bar{t}}$ background. The stacked histograms in the signal region at high m_{T} indicate the breakdown of the background predictions, mainly semileptonic and dileptonic $\mathrm{t\bar{t}}$ events.

For the signal regions with two OS leptons, Fig. 2 (bottom) shows a comparison of the m_{bb}

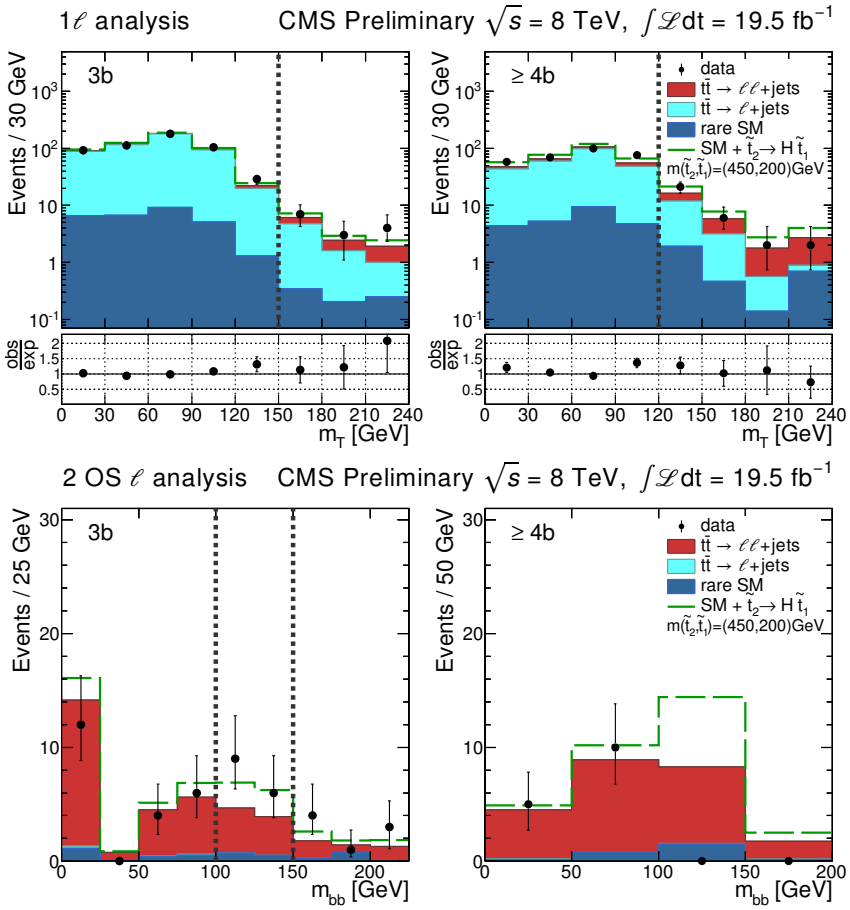

Figure 2: Comparison of the m_{T} distributions for events with one lepton (top row) and m_{bb} distributions for events with two OS leptons (bottom row) in data and MC simulation satisfying the 3b (left) and $\geq$ 4b (right) signal region requirements. The vertical dashed lines indicate the corresponding signal region requirement. The $\mathrm{t\bar{t}}$ simulation yields are adjusted so that the total SM prediction is normalized to the data in the samples obtained by inverting the signal region requirements. The distribution for the model $\tilde{\mathrm{t}}_2 \to \mathrm{H}\tilde{\mathrm{t}}_1$ where $m_{\tilde{\mathrm{t}}_2} = 450$ GeV and $m_{\tilde{\mathrm{t}}_1} = 200$ GeV is stacked on top of the backgrounds. The last bin contains the overflow. The uncertainties on the background predictions are derived for the total yields in the signal regions and are listed in Table 2.

distribution in data and simulation. The sample in the region outside the m_{bb} signal window is used to derive the normalization for the $\mathrm{t\bar{t}} \to \ell\ell +$ jets background prediction for events with three b jets. In the case of events with at least four b jets, multiple bb pairs are possible. The control region is not indicated in Fig. 2 (bottom right) since the m_{bb} requirement is not applied when $N_{\mathrm{bb}} > 1$. The stacked histograms indicate the breakdown of the background prediction, which is dominated by $\mathrm{t\bar{t}} \to \ell\ell +$ jets events. The results for the search regions with one lepton or two OS leptons are summarized in Table 2. The predicted and observed yields agree within about two standard deviations, given the statistical uncertainty on the data event yields.

For the baseline event selection with two SS leptons, Fig. 3 shows a comparison of data and the predicted backgrounds for three selection observables, the jet and b jet multiplicities and $E_{\mathrm{T}}^{\mathrm{miss}}$. The signal selection criteria are based on these variables (see Table 1) and give rise to regions ranging from tens of background events to regions with essentially no background,

also depending on the H_T requirement. The stacked histograms indicate the breakdown of the background predictions. The relative contribution from rare SM processes increases as the requirements are tightened. As shown in Table 3, the SM background predictions and observations are in agreement for both the high-p_T and low-p_T selections.

Finally, for the event sample with at least three leptons, Fig. 4 shows a comparison of data and the predicted backgrounds for three selection observables: the jet and b jet multiplicities, and E_T^{miss}. The stacked histograms indicate the breakdown of the background predictions. The dominant background is from processes with two prompt leptons and additional non-prompt

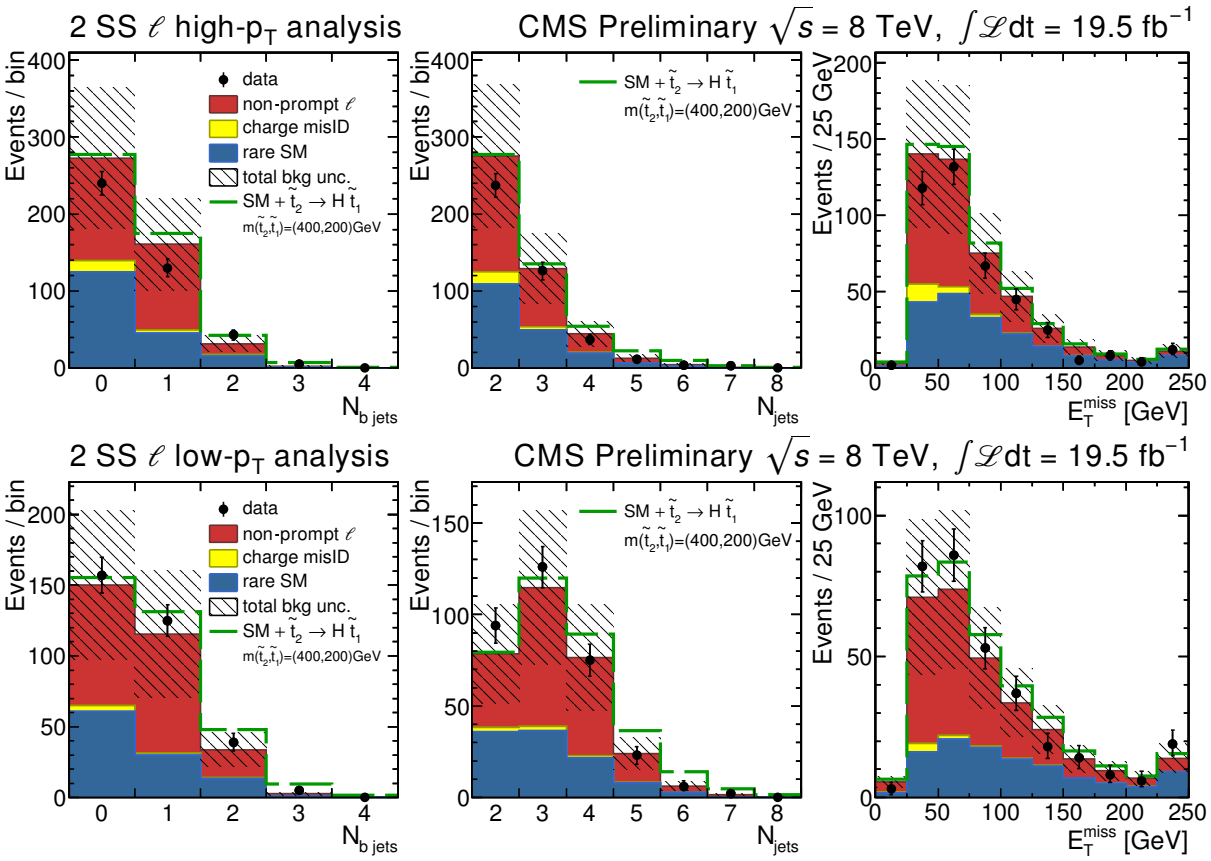

Figure 3: Data and predicted SM background for the event sample with two SS leptons as a function of number of jets, number of b jets and E_T^{miss} for events satisfying the high-p_T (top row) or the low-p_T (bottom row) selection. The shaded bands correspond to the total estimated uncertainty on the background prediction. The distribution for the model $\tilde{t}_2 \to H\tilde{t}_1$ where $m_{\tilde{t}_2} = 400$ GeV and $m_{\tilde{t}_1} = 200$ GeV is stacked on top of the backgrounds. The last bin in the histograms includes overflow events.

Table 2: Selection with one lepton or two OS leptons: background predictions and observed data yields. The uncertainties on the total background predictions include both the statistical and systematic components.

$N_{b\ jets}$	N_{jets}	E_T^{miss} [GeV]	1ℓ high m_T		2ℓ and bb requirement	
			Bkg.	Obs.	Bkg.	Obs.
$= 3$	≥ 5	≥ 50	10.0 ± 1.8	14	8.4 ± 2.7	15
≥ 4	≥ 4		27 ± 6	31	11 ± 5	3

Table 3: Same-sign dilepton selection: predicted total background and observed data yields as a function of the jet and b jet multiplicities, as well as the $E_{\mathrm{T}}^{\mathrm{miss}}$ and H_{T} requirements in units of GeV, for the low-p_{T} and high-p_{T} regions. The uncertainties on the total background predictions contain the statistical and systematic components.

Selection			low-p_{T}				high-p_{T}			
$N_{\mathrm{b\ jets}}$	N_{jets}	$E_{\mathrm{T}}^{\mathrm{miss}}$ [GeV]	$H_{\mathrm{T}} \in [250, 400]$ GeV		$H_{\mathrm{T}} \geq 400$ GeV		$H_{\mathrm{T}} \in [200, 400]$ GeV		$H_{\mathrm{T}} \geq 400$ GeV	
			Bkg.	Obs.	Bkg.	Obs.	Bkg.	Obs.	Bkg.	Obs.
$= 1$	2–3	50–120	29 ± 12	39	5.6 ± 2.0	5	31 ± 12	27	3.4 ± 1.2	5
		≥ 120	11 ± 4	8	4.9 ± 1.8	5	9.0 ± 3.2	9	3.5 ± 1.3	2
	≥ 4	50–120	15 ± 6	15	10 ± 4	6	9.2 ± 3.4	6	5.4 ± 2.0	2
		≥ 120	3.9 ± 1.5	3	6.1 ± 2.2	10	2.6 ± 1.0	3	3.5 ± 1.3	6
≥ 2	2–3	50–120	6.6 ± 2.4	10	1.3 ± 0.5	1	6.0 ± 2.1	11	0.78 ± 0.34	1
		≥ 120	2.4 ± 0.9	1	1.2 ± 0.5	2	2.4 ± 0.9	3	0.8 ± 0.4	1
	≥ 4	50–120	6.5 ± 2.5	5	4.0 ± 1.5	11	3.4 ± 1.3	2	2.3 ± 1.0	7
		≥ 120	1.8 ± 0.7	0	3.1 ± 1.2	3	1.1 ± 0.5	0	2.0 ± 0.8	2

Table 4: Predicted total background and observed data yields as a function of the jet and b jet multiplicities, as well as the $E_{\mathrm{T}}^{\mathrm{miss}}$ and H_{T} requirements in units of GeV, for events with at least three leptons, with (on-Z) and without (off-Z) a Z candidate present. The uncertainties on the total background predictions include both the statistical and systematic components.

Selection			off-Z				on-Z			
$N_{\mathrm{b\ jets}}$	N_{jets}	$E_{\mathrm{T}}^{\mathrm{miss}}$ [GeV]	$H_{\mathrm{T}} \in [60, 200]$ GeV		$H_{\mathrm{T}} \geq 200$ GeV		$H_{\mathrm{T}} \in [60, 200]$ GeV		$H_{\mathrm{T}} \geq 200$ GeV	
			Bkg.	Obs.	Bkg.	Obs.	Bkg.	Obs.	Bkg.	Obs.
$= 1$	2–3	50–100	34 ± 7	36	11.2 ± 2.5	9	16 ± 5	30	10 ± 4	13
		100–200	12.2 ± 2.7	13	9.1 ± 2.1	6	5.3 ± 1.8	6	5.9 ± 2.1	3
		≥ 200	0.33 ± 0.22	0	1.2 ± 0.5	0	0.37 ± 0.23	0	0.9 ± 0.4	0
	≥ 4	50–100	0.9 ± 0.4	2	5.4 ± 1.3	3	0.11 ± 0.13	1	5.0 ± 2.0	4
		100–200	0.10 ± 0.12	0	3.6 ± 1.0	3	0.08 ± 0.12	0	3.0 ± 1.3	5
		≥ 200	0.0 ± 0.1	0	0.76 ± 0.35	0	0.02 ± 0.10	0	0.56 ± 0.32	1
$= 2$	2–3	50–100	4.9 ± 1.2	7	3.9 ± 1.2	7	2.4 ± 0.9	5	2.5 ± 1.1	2
		100–200	2.3 ± 0.7	1	1.9 ± 0.7	0	1.3 ± 0.5	1	1.4 ± 0.6	1
		≥ 200	0.22 ± 0.21	1	0.14 ± 0.14	0	0.12 ± 0.13	0	0.43 ± 0.26	0
	≥ 4	50–100	0.03 ± 0.11	0	2.8 ± 0.9	1	0.20 ± 0.17	1	2.9 ± 1.3	1
		100–200	0.05 ± 0.11	0	1.7 ± 0.6	0	0.10 ± 0.13	0	1.7 ± 0.8	0
		≥ 200	0.0 ± 0.1	0	0.38 ± 0.21	0	0.0 ± 0.1	0	0.29 ± 0.19	0
≥ 3	≥ 3	50–100	0.0 ± 0.1	0	0.56 ± 0.27	1	0.0 ± 0.1	0	0.18 ± 0.15	0
		100–200	0.02 ± 0.11	0	0.18 ± 0.14	0	0.0 ± 0.1	0	0.25 ± 0.17	0
		≥ 200	0.0 ± 0.1	0	0.2 ± 0.2	0	0.0 ± 0.1	0	0.02 ± 0.10	0

leptons, mainly $\mathrm{t\bar{t}}$ events, though in the case of the on-Z selection, background sources with Z bosons also contribute significantly. The signal selection criteria are based on the variables in Fig. 4, as well as H_{T}, and give rise to event yields that range from tens of background events to low expected backgrounds. The results of the search, summarized in Table 4, show agreement between background predictions and observations for all the signal regions considered. In summary, the data yields are consistent with the background predictions across all channels and signal regions. Out of 96 signal regions, the largest discrepancy corresponds to a 1.6σ excess of local significance (30 observed compared to 16 ± 5 expected), computed following Ref. [57]. No indication of top-squark pairs is observed.

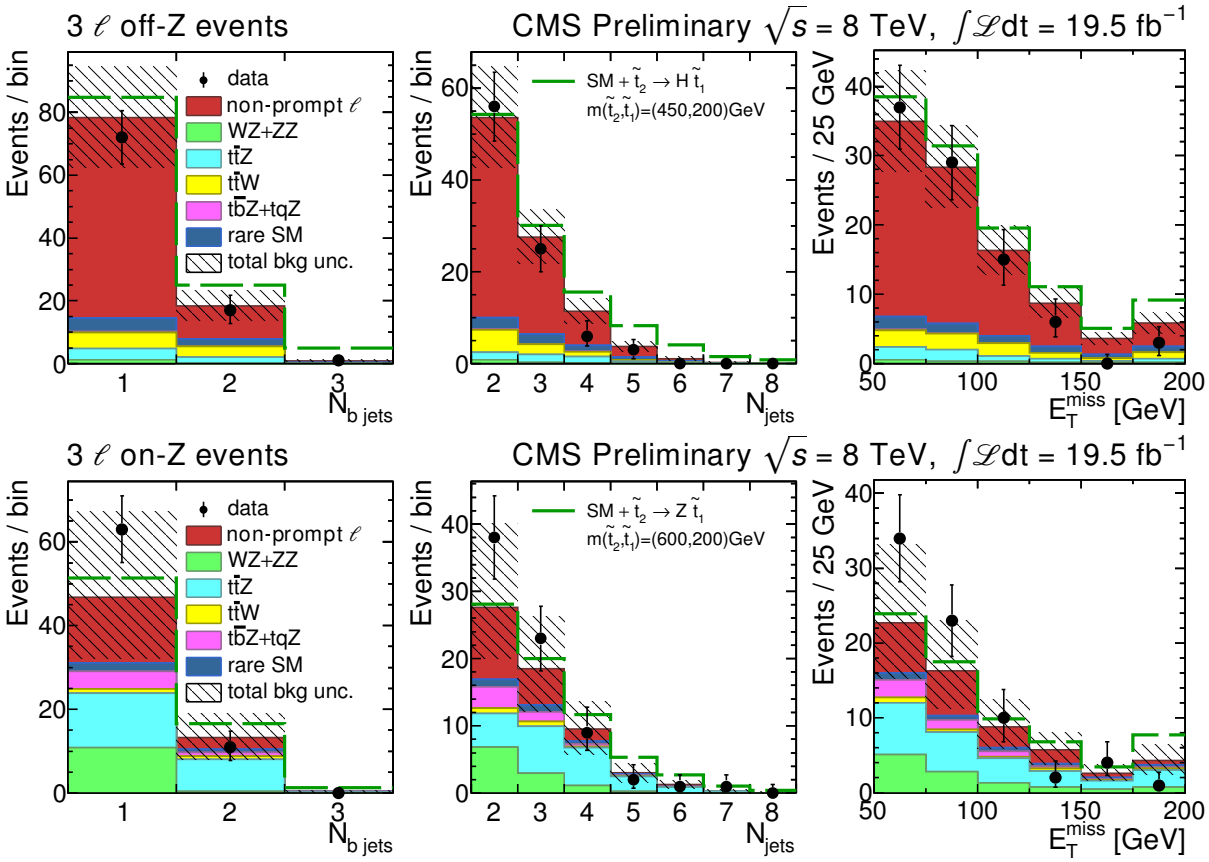

Figure 4: Observed data events and predicted SM background for the event sample with at least three leptons as a function of the number of jets, number of b jets and $E_{\mathrm{T}}^{\mathrm{miss}}$ are shown for events that do not contain (off-Z), top row, or contain (on-Z), bottom row, an opposite-sign-same-flavor pair that is a Z boson candidate. The distribution for the models $\tilde{t}_2 \to H\tilde{t}_1$ where $m_{\tilde{t}_2} = 450$ GeV and $m_{\tilde{t}_1} = 200$ GeV and $\tilde{t}_2 \to Z\tilde{t}_1$ where $m_{\tilde{t}_2} = 600$ GeV and $m_{\tilde{t}_1} = 200$ GeV are stacked on top of the backgrounds in the top and bottom rows respectively. The last bin in the histograms includes overflow events. The shaded bands correspond to the estimated uncertainties on the background which are calculated on the per bin basis.

6 Interpretation

In the absence of evidence for a signal, the results are used to set limits on the cross section times branching fraction for pair production of $\tilde{t}_2$ for the decay modes shown in Fig. 1. Upper limits on the pair production of $\tilde{t}_2$ are calculated at 95% confidence level (CL) using the LHC-style CL_S method [58, 59]. As explained below, the results from the various signal regions are combined in the limit setting procedure in order to improve the sensitivity of the search.

The limit calculation on the cross section times branching fraction depends on the signal selection efficiency and the background estimates. The signal regions with at least three leptons have the highest expected sensitivity because of the small amount of standard model background. For signal regions with at least three leptons, in the case of the $\mathrm{t\bar{t}HH}$ signal, off-Z search regions with high H_{T} ($H_{\mathrm{T}} > 200$ GeV) are used in the interpretation, while for the $\mathrm{t\bar{t}ZZ}$ case, both off-Z and on-Z search regions with high H_{T} are included. The total signal acceptance for all search regions with at least three leptons varies from around 0.4–0.5% for the $\mathrm{t\bar{t}HH}$ signal, to 1.2–1.5% for the $\mathrm{t\bar{t}ZZ}$ model. The acceptance for the most sensitive search region alone is around $\sim$0.1%

Table 5: Relative systematic uncertainties (in percent) on the signal for the different event selections: one lepton (1 ℓ), two OS leptons (2 OS ℓ), two SS leptons (2 SS ℓ), and at least three leptons (3 ℓ). The range indicates the variation in the systematic uncertainty for the different signal models and event kinematics selected in the signal regions considered.

Source	1 ℓ [%]	2 OS ℓ [%]	2 SS ℓ [%]	3 ℓ [%]
Luminosity [60]	2.6			
Pileup modeling	< 5			
Lepton identification and isolation efficiency	5	10	10	12
Trigger efficiency	3	6	6	5
Parton distribution functions	5	5	2	4
Jet energy scale modeling	1–3	1–3	1–10	5–15
b jet identification modeling	3–5	3–5	2–10	5–20
ISR modeling	3–5	3–5	3–15	3–15
Total	9–11	14–15	14–23	15–30

for $\mathrm{t\bar{t}HH}$ and approximately three times larger for $\mathrm{t\bar{t}ZZ}$. This difference in acceptance is because of the larger leptonic branching fraction for Z decays compared to H decays. The signal regions with lower lepton multiplicities also have sensitivity to the $\mathrm{t\bar{t}HH}$ signal. All search regions of the high–p_{T} SS dilepton analysis are used in the limit setting. While only the high–p_{T} results are used in the interpretation presented in this paper, the low–p_{T} experimental results are also included for use in other interpretations. The overall acceptance for $\mathrm{t\bar{t}HH}$ is 0.3–0.45%, where the most sensitive signal regions contribute $\sim$0.15%. In the case of signal regions with one lepton or two OS leptons, the acceptance for $\mathrm{t\bar{t}HH}$ is approximately 0.2–0.4%. The acceptances for the single lepton and dilepton final states are slightly lower in the $\mathrm{t\bar{t}ZZ}$ model. Because of this reduction, together with the large increase in acceptance for the trilepton final state, the single lepton and dilepton final states make a negligible contribution to the combination in the $\mathrm{t\bar{t}ZZ}$ model.

The sources of systematic uncertainty on the signal and their impact are listed in Table 5. The systematic uncertainties are evaluated in every search region and for every signal point separately. The total uncertainty on the signal selection efficiency is in the 9–30% range. The dominant source of uncertainty depends on the search region and model considered. An important source of uncertainty arises from the estimation of the trigger and lepton identification efficiencies, which are derived using $\mathrm{Z} \to \ell^+\ell^-$ samples, and contribute 6–13%. The uncertainty due the knowledge of the energy scale of hadronic jets increases with tighter kinematic requirements and corresponds to an uncertainty of 1–15%. For smaller mass differences between $m_{\tilde{\mathrm{t}}_2}$ and $m_{\tilde{\mathrm{t}}_1}$, the modeling of the initial-state radiation (ISR) is an important effect. The corresponding uncertainty in the signal selection efficiency is of 3–15%, increasing with smaller $\Delta(m_{\tilde{\mathrm{t}}_2}, m_{\tilde{\mathrm{t}}_1})$. The systematic uncertainties on the signal model, including their correlations, are treated consistently in the different analyses. The correlations between the different analyses have a small impact on the combined result. The systematic uncertainties and correlations are accounted for as nuisance parameters and are varied in ensemble tests according to log-normal distributions. The correlations on the background estimates are also are taken into account.

The exclusion curves on particle masses at 95% CL are evaluated from a comparison of the cross section upper limits and the theoretical signal cross section predictions. Figure 5 shows the 95% CL upper limits on the cross section times branching fraction in the $m_{\tilde{\mathrm{t}}_1}$ versus $m_{\tilde{\mathrm{t}}_2}$ plane for the (a) $\tilde{\mathrm{t}}_2 \to \mathrm{H}\tilde{\mathrm{t}}_1$ and (b) $\tilde{\mathrm{t}}_2 \to \mathrm{Z}\tilde{\mathrm{t}}_1$ decay modes. The contour bounds the excluded region

in the plane assuming the NLO+NLL cross section calculation in the decoupling limit for all the SUSY sparticles not included in the model. The results are presented assuming a branching fraction of 100% to each decay mode. The 95% CL expected (thick dashed red) and observed (solid black) limits are obtained including all uncertainties with the exception of the theoretical uncertainty on the signal production cross section. The expected limit is defined as the median of the upper limit distribution obtained using pseudo-experiments and the likelihood model considered. The bands around the expected limit correspond to the impact of experimental uncertainties on the limit, and the bands around the observed limit indicate the change for a $\pm 1\sigma$ variation in the theoretical cross section.

The results for the pure $\widetilde{t}_2 \to H\widetilde{t}_1$ decay (Fig. 5a right) show that the signal regions with at least three leptons, no $Z \to \ell^+\ell^-$ candidates, and large b jet multiplicities are the most sensitive. Nevertheless the signal regions with lower lepton multiplicities (one lepton or two leptons) have significant expected sensitivity in the $\widetilde{t}_2 \to H\widetilde{t}_1$ decay mode. Because of the dominant $H \to b\bar{b}$ decay mode, the higher b jet multiplicities dominate the expected sensitivity to signals with H bosons for every lepton multiplicity. Including the final states with lower lepton multiplicities in the combination lowers the cross section upper limit by 15–20% compared to the three lepton results alone. Therefore, all lepton categories are used in the interpretation of the $t\bar{t}HH$ signal.

In the case of the signals with Z bosons (Fig. 5b right), the signal regions with at least three leptons completely dominate the expected sensitivity. The different signal regions with at least three leptons provide sensitivity to different types of signal models. In particular, off-Z signal regions are sensitive to the region of parameter space in which the Z bosons are off-shell $m_{\widetilde{t}_2} - m_{\widetilde{t}_1} < m_Z$, while the on-Z regions provide sensitivity to signals with larger mass differences. In this decay mode, the selections with low b jet multiplicities are most sensitive. Only the signal regions with at least three leptons are used in the interpretation of the $t\bar{t}ZZ$ signal.

In the $\widetilde{t}_2 \to H\widetilde{t}_1$ decay mode, taking a -1σ theory lower bound on signal cross sections, a $\widetilde{t}_2$ with $m_{\widetilde{t}_2} \lesssim 525$ GeV is excluded at 95% CL for $\widetilde{t}_1$ with $m_{\widetilde{t}_1} \lesssim 300$ GeV. Similarly, in the $\widetilde{t}_2 \to Z\widetilde{t}_1$ decay mode, a $\widetilde{t}_2$ with $m_{\widetilde{t}_2} \lesssim 575$ GeV is excluded at 95% CL for $\widetilde{t}_1$ with $m_{\widetilde{t}_1} \lesssim 400$ GeV.

Mixed-decay scenarios, with non-zero branching fractions for the Z and H decay modes are also considered, assuming these are the only decay modes possible. Figure 6 shows the corresponding limits as a function of the relative branching fraction of the Z and H decay modes. The scenario with the least expected sensitivity is where the H decay mode dominates, while the best expected sensitivity is achieved when the Z decay mode dominates.

The cross section limits are obtained neglecting the contribution of direct $\widetilde{t}_1$ pair production. Including this additional contribution in the single lepton or two OS lepton signal regions, which can satisfy the multi-b event selection due to the mistag of light-parton jets or due to additional b jets from radiation, typically lowers the cross section limit by a few percent, increasing with $\widetilde{t}_2$ mass. The contribution in the case of events with two SS leptons or at least three leptons is small due to the low probability of misidentifying non-prompt leptons. Since the signature with three leptons has the best sensitivity overall, the impact on the combined limit is much smaller than the uncertainty on the production cross section.

7 Summary

This paper presents results from a search for pair production of the heavier top-squark mass eigenstate $\widetilde{t}_2$ decaying to the lighter eigenstate $\widetilde{t}_1$ and producing a signature of $t\bar{t}$ in associa-

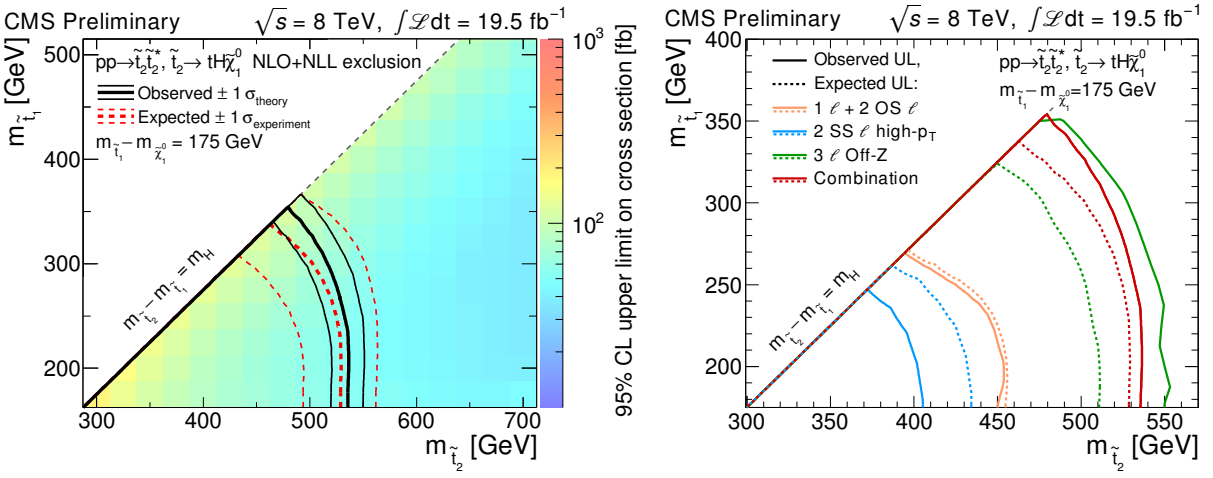

(a) Combined result $\tilde{t}_2 \to H\tilde{t}_1$.

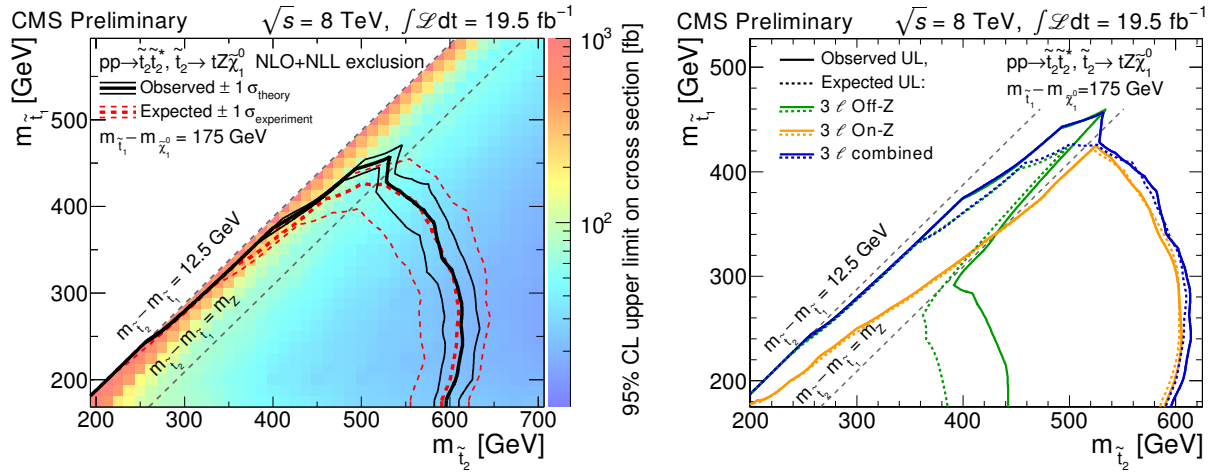

(b) Combined result $\tilde{t}_2 \to Z\tilde{t}_1$.

Figure 5: The distributions on the left show the 95% CL upper limits (UL) on the cross section times branching fraction of $\tilde{t}_2$ pair production in the decay mode (a) $\tilde{t}_2 \to H\tilde{t}_1$ and (b) $\tilde{t}_2 \to Z\tilde{t}_1$ in the plane of $m_{\tilde{t}_1}$ versus $m_{\tilde{t}_2}$ assuming NLO+NLL cross section. The $\tilde{t}_1$ is assumed to decay to top plus neutralino assuming $m_{\tilde{t}_1} - m_{\tilde{\chi}_1^0} = m_t$. A branching fraction of unity is assumed for each decay mode. The black (red) curves indicate the observed (expected) exclusion contours for the combination of the three event categories. The $\pm 1\sigma$ bands are indicated by the finer contours. The distributions on the right show the observed (expected) exclusion contours indicated by the solid (dashed) curves for the contributing analyses for the different decay modes and the combination. In (a), the red curves indicate the combination of the three event categories for the $\tilde{t}_2 \to H\tilde{t}_1$ signal, while in (b), the blue curves indicate the combination of the on-Z and off-Z analyses for events with at least three leptons.

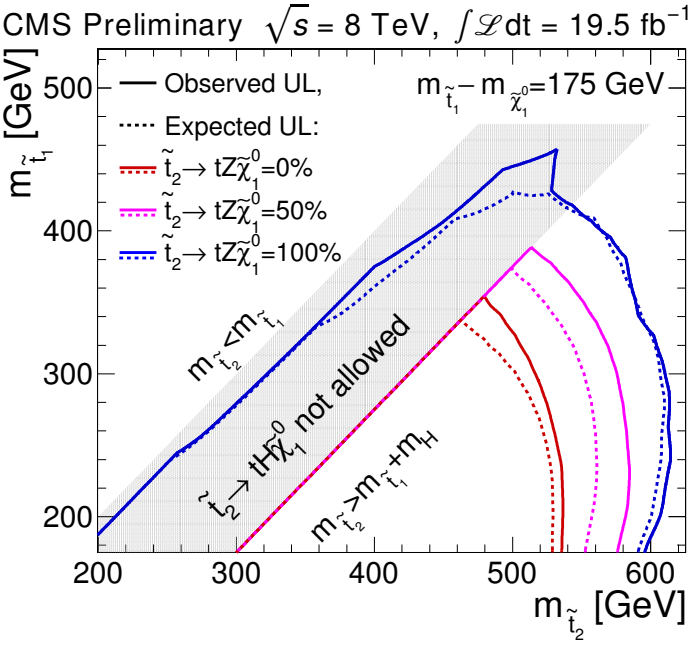

Figure 6: Upper limits on the production cross section of $\tilde{t}_2$ pair production for different branching fractions of $\tilde{t}_2 \to H\tilde{t}_1$ and $\tilde{t}_2 \to Z\tilde{t}_1$. The $\tilde{t}_1$ is assumed to decay to top quark plus neutralino assuming $m_{\tilde{t}_1} - m_{\tilde{\chi}_1^0} = m_t$. The decay $\tilde{t}_2 \to H\tilde{t}_1$ is only considered when the H boson production is kinematically allowed, $m_{\tilde{t}_2} - m_{\tilde{t}_1} > m_H$.

tion with H or Z bosons. The analyses explore final states with one lepton or two leptons of opposite-sign charge accompanied by at least three b jets, and two leptons of the same-sign charge or at least three leptons accompanied by at least one b jet. No significant excess event yield above SM expectations is observed. The results are used to exclude a range of $\tilde{t}_2$ masses below approximately 575 GeV for $\tilde{t}_1$ masses below approximately 400 GeV, assuming $\tilde{t}_1$ always decays to $t\tilde{\chi}_1^0$ and that $m_{\tilde{t}_1} - m_{\tilde{\chi}_1^0} \sim m_t$. This is a region of phase not probed in existing searches for direct top-squark pair production.

References

[1] S. Dimopoulos and S. Raby, "Supercolor", *Nucl. Phys. B* **192** (1981) 353, doi:10.1016/0550-3213(81)90430-2.

[2] E. Witten, "Dynamical Breaking of Supersymmetry", *Nucl. Phys. B* **188** (1981) 513, doi:10.1016/0550-3213(81)90006-7.

[3] M. Dine, W. Fischler, and M. Srednicki, "Supersymmetric Technicolor", *Nucl. Phys. B* **189** (1981) 575, doi:10.1016/0550-3213(81)90582-4.

[4] S. Dimopoulos and H. Georgi, "Softly Broken Supersymmetry and SU(5)", *Nucl. Phys. B* **193** (1981) 150, doi:10.1016/0550-3213(81)90522-8.

[5] N. Sakai, "Naturalness in Supersymmetric Guts", *Z. Phys. C* **11** (1981) 153, doi:10.1007/BF01573998.

[6] R. K. Kaul and P. Majumdar, "Cancellation of quadratically divergent mass corrections in globally supersymmetric spontaneously broken gauge theories", *Nucl. Phys. B* **199** (1982) 36, doi:10.1016/0550-3213(82)90565-X.

[7] R. Barbieri and G. F. Giudice, "Upper bounds on supersymmetric particle masses", *Nucl. Phys. B* **306** (1988) 63, doi:10.1016/0550-3213(88)90171-X.

[8] B. de Carlos and J. A. Casas, "One-loop analysis of the electroweak breaking in supersymmetric models and the fine-tuning problem", *Phys. Lett. B* **309** (1993) 320, doi:10.1016/0370-2693(93)90940-J, arXiv:hep-ph/9303291.

[9] S. Dimopoulos and G. F. Giudice, "Naturalness constraints in supersymmetric theories with non-universal soft terms", *Phys. Lett. B* **357** (1995) 573, doi:10.1016/0370-2693(95)00961-J, arXiv:hep-ph/9507282.

[10] R. Barbieri, G. Dvali, and L. J. Hall, "Predictions from a U(2) flavour symmetry in supersymmetric theories", *Phys. Lett. B* **377** (1996) 76, doi:10.1016/0370-2693(96)00318-8, arXiv:hep-ph/9512388.

[11] M. Papucci, J. T. Ruderman, and A. Weiler, "Natural SUSY Endures", *JHEP* **09** (2012) 035, doi:10.1007/JHEP09(2012)035, arXiv:1110.6926.

[12] ATLAS Collaboration, "Search for a supersymmetric partner to the top quark in final states with jets and missing transverse momentum at $\sqrt{s} = 7$ TeV with the ATLAS detector", *Phys. Rev. Lett.* **109** (2012) 211802, doi:10.1103/PhysRevLett.109.211802, arXiv:1208.1447.

[13] ATLAS Collaboration, "Search for direct top squark pair production in final states with one isolated lepton, jets, and missing transverse momentum in $\sqrt{s} = 7$ TeV pp collisions using 4.7 fb^{-1} of ATLAS data", *Phys. Rev. Lett.* **109** (2012) 211803, doi:10.1103/PhysRevLett.109.211803, arXiv:1208.2590.

[14] ATLAS Collaboration, "Search for light scalar top quark pair production in final states with two leptons with the ATLAS detector in $\sqrt{s} = 7$ TeV proton-proton collisions", *Eur. Phys. J. C* **72** (2012) 2237, doi:10.1140/epjc/s10052-012-2237-1, arXiv:1208.4305.

[15] ATLAS Collaboration, "Search for light top squark pair production in final states with leptons and b-jets with the ATLAS detector in $\sqrt{s} = 7$ TeV proton-proton collisions", *Phys. Lett. B* **720** (2013) 13, doi:10.1016/j.physletb.2013.01.049, arXiv:1209.2102.

[16] CMS Collaboration, "Search for top-squark pair production in the single-lepton final state in pp collisions at $\sqrt{s} = 8$ TeV", *Eur. Phys. J. C* **73** (2013) 2677, doi:10.1140/epjc/s10052-013-2677-2, arXiv:1308.1586.

[17] Z. Han, A. Katz, D. Krohn, and M. Reece, "(Light) Stop Signs", *JHEP* **1208** (2012) 083, doi:10.1007/JHEP08(2012)083, arXiv:1205.5808.

[18] CMS Collaboration, "Search for supersymmetry in pp collisions at $\sqrt{s} = 8$ TeV in events with a single lepton, large jet multiplicity, and multiple b jets", (2013). arXiv:1311.4937. Submitted to *Phys. Lett. B*.

[19] CMS Collaboration, "Search for gluino mediated bottom- and top-squark production in multijet final states in pp collisions at 8 TeV", *Phys. Lett. B* **725** (2013) 243–270, doi:10.1016/j.physletb.2013.06.058, arXiv:1305.2390.

[20] ATLAS Collaboration, "Search for scalar top quark pair production in natural gauge mediated supersymmetry models with the ATLAS detector in pp collisions at $\sqrt{s} = 7$ TeV", *Phys. Lett. B* **715** (2012) 44, doi:10.1016/j.physletb.2012.07.010, arXiv:1204.6736.

[21] CMS Collaboration, "Study of tau reconstruction algorithms using pp collisions data collected at $\sqrt{s} = 7$ TeV", CMS Physics Analysis Summary CMS-PAS-PFT-10-004, 2010.

[22] CMS Collaboration, "CMS strategies for tau reconstruction and identification using particle-flow techniques", CMS Physics Analysis Summary CMS-PAS-PFT-08-001, 2009.

[23] CMS Collaboration, "Electron reconstruction and identification at $\sqrt{s} = 7$ TeV", CMS Physics Analysis Summary CMS-PAS-EGM-10-004, 2010.

[24] CMS Collaboration, "Performance of CMS muon reconstruction in pp collision events at $\sqrt{s} = 7$ TeV", *JINST* **7** (2012) P10002, doi:10.1088/1748-0221/7/10/P10002, arXiv:1206.4071.

[25] CMS Collaboration, "Evidence for the 125 GeV Higgs boson decaying to a pair of τ leptons", (2014). arXiv:1401.5041. Submitted to *JHEP*.

[26] M. Cacciari, G. P. Salam, and G. Soyez, "The anti-k_T jet clustering algorithm", *JHEP* **04** (2008) 063, doi:10.1088/1126-6708/2008/04/063, arXiv:0802.1189.

[27] CMS Collaboration, "Determination of jet energy calibration and transverse momentum resolution in CMS", *JINST* **6** (2011) P11002, doi:10.1088/1748-0221/6/11/P11002, arXiv:1107.4277.

[28] M. Cacciari and G. P. Salam, "Pileup subtraction using jet areas", *Phys. Lett. B* **659** (2008) 119, doi:10.1016/j.physletb.2007.09.077, arXiv:0707.1378.

[29] CMS Collaboration, "Identification of b-quark jets with the CMS experiment", *JINST* **8** (2013) P04013, doi:10.1088/1748-0221/8/04/P04013, arXiv:1211.4462.

[30] J. Alwall et al., "MadGraph 5 : Going Beyond", *JHEP* **06** (2011) 128, doi:10.1007/JHEP06(2011)128, arXiv:1106.0522.

[31] T. Sjöstrand, S. Mrenna, and P. Skands, "PYTHIA 6.4 physics and manual", *JHEP* **05** (2006) 026, doi:10.1088/1126-6708/2006/05/026, arXiv:hep-ph/0603175.

[32] CMS Collaboration, "Interpretation of Searches for Supersymmetry with simplified Models", *Phys. Rev. D* **88** (2013) 052017, doi:10.1103/PhysRevD.88.052017, arXiv:1301.2175.

[33] CMS Collaboration, "Observation of a new boson at a mass of 125 GeV with the CMS experiment at the LHC", *Phys. Lett. B* **716** (2012) 30, doi:10.1016/j.physletb.2012.08.021, arXiv:1207.7235.

[34] S. Dittmaier et al., "Handbook of LHC Higgs Cross Sections: 2. Differential Distributions", (2012). arXiv:1201.3084.

[35] W. Beenakker, R. Höpker, M. Spira, and P. M. Zerwas, "Squark and gluino production at hadron colliders", *Nucl. Phys. B* **492** (1997) 51, doi:10.1016/S0550-3213(97)00084-9, arXiv:hep-ph/9610490.

[36] A. Kulesza and L. Motyka, "Threshold resummation for squark-antisquark and gluino-pair production at the LHC", *Phys. Rev. Lett.* **102** (2009) 111802, doi:10.1103/PhysRevLett.102.111802, arXiv:0807.2405.

[37] A. Kulesza and L. Motyka, "Soft gluon resummation for the production of gluino-gluino and squark-antisquark pairs at the LHC", *Phys. Rev. D* **80** (2009) 095004, doi:10.1103/PhysRevD.80.095004, arXiv:0905.4749.

[38] W. Beenakker et al., "Soft-gluon resummation for squark and gluino hadroproduction", *JHEP* **12** (2009) 041, doi:10.1088/1126-6708/2009/12/041, arXiv:0909.4418.

[39] W. Beenakker et al., "Squark and gluino hadroproduction", *Int. J. Mod. Phys. A* **26** (2011) 2637, doi:10.1142/S0217751X11053560, arXiv:1105.1110.

[40] M. Kramer et al., "Supersymmetry production cross sections in pp collisions at $\sqrt{s} = 7$ TeV", (2012). arXiv:1206.2892.

[41] S. Frixione, P. Nason, and C. Oleari, "Matching NLO QCD computations with parton shower simulations: the POWHEG method", *JHEP* **11** (2007) 070, doi:10.1088/1126-6708/2007/11/070, arXiv:0709.2092.

[42] S. Frixione and B. R. Webber, "Matching NLO QCD computations and parton shower simulations", *JHEP* **06** (2002) 029, arXiv:hep-ph/0204244.

[43] S. Frixione, P. Nason, and B. R. Webber, "Matching NLO QCD and parton showers in heavy flavor production", *JHEP* **08** (2003) 007, arXiv:hep-ph/0305252.

[44] H.-L. Lai et al., "New parton distributions for collider physics", *Phys. Rev. D* **82** (2010) 074024, doi:10.1103/PhysRevD.82.074024, arXiv:1007.2241.

[45] J. Pumplin et al., "New generation of parton distributions with uncertainties from global QCD analysis", *JHEP* **07** (2002) 012, arXiv:hep-ph/0201195.

[46] N. Kidonakis, "Differential and total cross sections for top pair and single top production", doi:10.3204/DESY-PROC-2012-02/251, arXiv:1205.3453.

[47] J. M. Campbell and R. K. Ellis, "$t\bar{t}W^{\pm}$ production and decay at NLO", *JHEP* **07** (2012) 052, doi:10.1007/JHEP07(2012)052, arXiv:1204.5678.

[48] M. Garzelli, A. Kardos, C. Papadopoulos, and Z. Trocsanyi, "$t\bar{t}W^{\pm}$ and $t\bar{t}Z$ Hadroproduction at NLO Accuracy in QCD with Parton Shower and Hadronization Effects", *JHEP* **11** (2012) 056, doi:10.1007/JHEP11(2012)056, arXiv:1208.2665.

[49] J. M. Campbell and R. Ellis, "MCFM for the Tevatron and the LHC", *Nucl. Phys. Proc. Suppl.* **205-206** (2010) 10, doi:10.1016/j.nuclphysbps.2010.08.011, arXiv:1007.3492.

[50] R. Gavin, Y. Li, F. Petriello, and S. Quackenbush, "W Physics at the LHC with FEWZ 2.1", *Comput. Phys. Commun.* **184** (2013) 208, doi:10.1016/j.cpc.2012.09.005, arXiv:1201.5896.

[51] R. Frederix et al., "Four-lepton production at hadron colliders: aMC@NLO predictions with theoretical uncertainties", *JHEP* **02** (2012) 099, doi:10.1007/JHEP02(2012)099, arXiv:1110.4738.

[52] CMS Collaboration, "The fast simulation of the CMS detector at LHC", *J. Phys. Conf. Ser.* **331** (2011) 032049, doi:10.1088/1742-6596/331/3/032049.

[53] GEANT4 Collaboration, "GEANT4 – a simulation toolkit", *Nucl. Instrum. Meth. A* **506** (2003) 250, doi:10.1016/S0168-9002(03)01368-8.

[54] CMS Collaboration, "Performance of τ lepton reconstruction and identification in CMS", *JINST* **7** (2012) P01001, doi:10.1088/1748-0221/7/01/P01001, arXiv:1109.6034.

[55] CMS Collaboration, "Search for new physics in events with same-sign dileptons and jets in pp collisions at 8 TeV", *JHEP* **01** (2014) 163, doi:10.1007/JHEP01(2014)163, arXiv:1311.6736.

[56] CMS Collaboration, "Measurement of associated production of vector bosons and top quark-antiquark pairs at sqrt(s) = 7 TeV", *Phys. Rev. Lett.* **110** (2013) 172002, doi:10.1103/PhysRevLett.110.172002, arXiv:1303.3239.

[57] R. D. Cousins, J. T. Linnemann, and J. Tucker, "Evaluation of three methods for calculating statistical significance when incorporating a systematic uncertainty into a test of the background-only hypothesis for a Poisson process", *Nucl. Instrum. Meth. A* **595** (2008) 480, doi:10.1016/j.nima.2008.07.086, arXiv:physics/0702156.

[58] T. Junk, "Confidence level computation for combining searches with small statistics", *Nucl. Instrum. Meth. A* **434** (1999) 435, doi:10.1016/S0168-9002(99)00498-2, arXiv:hep-ex/9902006.

[59] A. L. Read, "Presentation of search results: the CL_S technique", *J. Phys. G* **28** (2002) 2693, doi:10.1088/0954-3899/28/10/313.

[60] CMS Collaboration, "CMS luminosity based on pixel cluster counting — Summer 2013 update", CMS Physics Analysis Summary CMS-PAS-LUM-13-001, 2013.